



ОБЪЕДИНЕННЫЙ
ИНСТИТУТ
ЯДЕРНЫХ
ИССЛЕДОВАНИЙ
ДУБНА

377-93

E4-93-377

G.G.Adamian, N.V.Antonenko, R.V.Jolos,
S.P.Ivanova, O.I.Melnikova

POTENTIAL ENERGY
OF DINUCLEAR SYSTEM

Submitted to "Ядерная физика"

1993

1. Introduction

The dinuclear system (DNS) formation in deep inelastic heavy ion collisions is well known [1]. The charge and mass distributions of reaction products are predicted mainly by the DNS evolution. The relationship between the fusion and quasi-fission processes depends on the initial DNS configuration. To describe the DNS dynamics, we need the calculation of the DNS potential energy at different values of its charge (mass) asymmetry, distance R between the centers of nuclei, nuclei deformations and angular momentum J . A small overlap of the nuclei of DNS allows us to write down the potential energy as a sum of the binding energies of both nuclei (B_1 and B_2) and the energy of their interaction. The nucleus-nucleus potential

$$U(R) = U_N(R) + U_{coul}(R) + U_{rot}(R) \quad (1)$$

is a sum of nuclear, Coulomb and centrifugal potentials. Usually, the calculation of $U_N(R)$ is most difficult in (1).

Different versions of the potential $U_N(R)$ describing the elastic scattering and reaction cross section in heavy ion reactions can be found in the literature [2]. However, they have a limited range of applicability. For instance, the energy density formalism [3] gives a too large value of the distance between the barrier position R_b and the position of the potential pocket minimum R_m . This corresponds to a considerable overlap of nuclei. The proximity potential [4] is good enough for the description of interaction of medium and heavy nuclei. However, for strongly asymmetric DNS its application is not valid. In this case the proximity potential leads to a very deep potential pocket and contradictory results since the absolute value of the potential minimum is essentially larger than the Q -reaction value.

A detailed analysis [5] of various theoretical schemes testifies great efficiency of the folding procedure of nucleon-nucleon interaction with the nucleon densities of colliding nuclei to construct $U_N(R)$. The question is which nucleon-nucleon forces are most preferable for the calculations. By using the density independent nucleon-nucleon interaction, a very deep nucleus-nucleus potential can be obtained. These potentials are used, for example, to describe α -decay. It is assumed that an α -particle is located on the first nonoccupied level since the transition to lower levels are forbidden by the Pauli principle. However, the Pauli principle can effectively be taken into account by the repulsive core in the potential. In this case the potential has a small depth and few bound states in it. In the framework of the microscopical approach the

repulsive core appears because of the antisymmetrization effect. The same physical results can be obtained by using both the deep potential and the potential with the repulsive core. However, to simplify the calculation of the DNS potential energy, the second one should be used, especially in the case of interaction of massive nuclei. An investigation of the DNS evolution necessitates the potential energy calculation for various DNS configurations. Nevertheless, the method of calculation of the nucleus-nucleus potential should be available both for symmetric and for asymmetric systems.

In view of the planned investigations of the exotic nuclear shapes and nuclear reactions with radioactive beams the calculation of the DNS potential energy for its various characteristics is an important problem. It is interesting also to find nuclear systems where the states with exotic shapes (cluster type states) can appear at relatively low excitation energies. Light nuclei emission from the contact region of two heavy nuclei [6] can be an indication of the existence of trinuclear systems. Moreover, the energy of some symmetric DNS seems to be close to the energy of the corresponding compound nucleus. In this case the nucleus can transform into the DNS configuration at a low excitation energy.

In this paper we shall obtain the expressions which are convenient for the calculation of the double folding nucleus-nucleus potential [7]. The interaction of spherical and deformed nuclei will be considered. The relationship between the proposed potential $U_N(R)$ and proximity potential will be found out. The results obtained will be applied to the calculation of the potential energy of real DNS.

2. Nucleus-nucleus potential

2.1 NUCLEAR INTERACTION

The repulsive core in the double folding potential

$$U_N(R) = \int \rho_1(\mathbf{r}_1)\rho_2(\mathbf{R} - \mathbf{r}_2)\mathcal{F}(\mathbf{r}_1 - \mathbf{r}_2)d\mathbf{r}_1d\mathbf{r}_2 \quad (2)$$

is obtained naturally when one uses density-dependent nucleon-nucleon forces [8]:

$$\begin{aligned} \mathcal{F}(\mathbf{r}_1 - \mathbf{r}_2) &= C_0 \left(F_{in} \frac{\rho_0(\mathbf{r}_1)}{\rho_{00}} + F_{ex} \left(1 - \frac{\rho_0(\mathbf{r}_1)}{\rho_{00}} \right) \right) \delta(\mathbf{r}_1 - \mathbf{r}_2), \\ F_{in,ex} &= (f_{in,ex} + f'_{in,ex} \tau_1 \tau_2) + g_{in,ex} + g'_{in,ex} \tau_1 \tau_2 \sigma_1 \sigma_2. \end{aligned} \quad (3)$$

Here σ_i and τ_i are spin and isospin matrices, respectively. The value of C_0 and the dimensionless parameters f , f' , g and g' are known from the description of a large set of experimental data within the theory of finite Fermi systems [8]. The interaction (3)

is similar to the density-dependent Skyrme one [9]. At a small overlap of nuclei and retaining their individuality during the interaction [10] the nucleon density of DNS can be written in the sudden approximation

$$\rho_0(\mathbf{r}) = \rho_1(\mathbf{r}) + \rho_2(\mathbf{r}), \quad (4)$$

where $\rho_i(\mathbf{r})$ ($i = 1, 2$) are the nucleon densities of interacting nuclei. If one neglects the spin dependence in (3), then (2) can be rewritten as

$$\begin{aligned} U_N(R) &= C_0 \left\{ \frac{F_{in} - F_{ex}}{\rho_{00}} \left(\int \rho_1^2(\mathbf{r}) \rho_2(\mathbf{r} - \mathbf{R}) d\mathbf{r} \right. \right. \\ &\quad \left. \left. + \int \rho_1(\mathbf{r}) \rho_2^2(\mathbf{r} - \mathbf{R}) d\mathbf{r} \right) + F_{ex} \int \rho_1(\mathbf{r}) \rho_2(\mathbf{r} - \mathbf{R}) d\mathbf{r} \right\}, \quad (5) \\ F_{in,ex} &= f_{in,ex} + f'_{in,ex} (N_1 - Z_1)/A_1 \cdot (N_2 - Z_2)/A_2, \end{aligned}$$

where N_i , Z_i and A_i are neutron, proton and mass numbers, respectively. When one considers the interaction of nuclei with mass numbers $A_i > 16$, the nuclear density can be taken either in the Saxon-Woods dependence

$$\rho_i(\mathbf{r}) = \frac{\rho_{00}}{1 + \exp((r - R_i(\theta'_i, \varphi'_i))/a_{0i})} \quad (6)$$

or in its symmetric form

$$\rho_i(\mathbf{r}) = \frac{\rho_{00} \sinh(R_i(\theta'_i, \varphi'_i)/a_{0i})}{\cosh(R_i(\theta'_i, \varphi'_i)/a_{0i}) + \cosh(r/a_{0i})}. \quad (7)$$

Near the nuclear surface the dependences (6) and (7) are close to each other. The contact region of two nuclei is the one giving a main contribution to the integrals of (5). A simpler Fourier transform of function (7) facilitates the calculation of the integrals in (5). In the expressions (6) and (7) R_i and a_{0i} denote the radius and diffuseness of i th nucleus, respectively, $\rho_{00} = 0.17 \text{ fm}^{-3}$. For light spherical nuclei the more realistic functional dependence of $\rho_i(r)$ on r is the following

$$\rho_i(\mathbf{r}) = A_i (\gamma^2/\pi)^{3/2} \exp(-\gamma^2 r^2), \quad (8)$$

where γ characterizes the width of the nucleon distribution in the nucleus [11–13]. The value of γ can be obtained by minimizing the nuclear binding energy in the density functional.

Without restricting the general nature of further calculations let us consider for simplicity only the quadrupole deformed, axial symmetric nuclei

$$R_i = R_{0i} (1 + \beta_i Y_{20}(\theta'_i, \varphi'_i)), \quad (9)$$

where $R_{0i} = r_0 A_i^{1/3}$ and angles (θ'_i, φ'_i) are in the body-fixed system. The rotation of its axes is described by the Euler angles Ω_i with respect to the space-fixed system. The axis z of the space-fixed system coincides with \mathbf{R} (Fig.1).

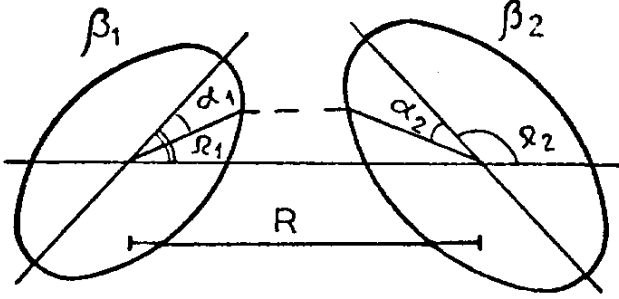


Fig.1. Schematic configuration of two axially symmetric deformed nuclei

It is known that the expansion of (6) and (7) in the deformation parameter β_i converges well at small β_i . For $\beta_i > 0.2$ the following modified expansions suit better for calculations

$$\rho_i(\mathbf{r}) \simeq \rho_i(r) + \xi_i \left[R_{0i} \frac{d\tilde{\rho}_i(r)}{dR_{0i}} \beta_i Y_{20}(\theta'_i) + \frac{R_{0i}^2}{2} \frac{d^2\tilde{\rho}_i(r)}{dR_{0i}^2} \beta_i^2 Y_{20}^2(\theta'_i) \right], \quad (10)$$

$$\rho_i^2(\mathbf{r}) \simeq \rho_i^2(r) + \xi'_i \left[R_{0i} \frac{d\tilde{\rho}_i^2(r)}{dR_{0i}} \beta_i Y_{20}(\theta'_i) + \frac{R_{0i}^2}{2} \frac{d^2\tilde{\rho}_i^2(r)}{dR_{0i}^2} \beta_i^2 Y_{20}^2(\theta'_i) \right], \quad (11)$$

where $\tilde{\rho}_i(r)$ and $\tilde{\rho}_i^2(r)$ differ from $\rho_i(r)$ and $\rho_i^2(r)$ by the replacement of a_{0i} by b_{0i} and b'_{0i} , respectively. The values of ξ_i , ξ'_i , b_{0i} and b'_{0i} are fixed by fitting the radial dependences of $\rho_i(r)$ and $\rho_i^2(r)$ at $\theta'_i = \alpha_i$. The angle α_i corresponds to the nuclear surface point nearest to the other nucleus (Fig.1). A small overlap of nuclei allows one to neglect the dependence of coefficients in (10) and (11) on θ'_i .

Let us consider the first integral in (5)

$$I_1 = \int \rho_1^2(\mathbf{r}) \rho_2(\mathbf{r} - \mathbf{R}) d\mathbf{r} = \sum_{k=1}^9 I_{1k}. \quad (12)$$

Inserting the Fourier transformations and using the expression

$$\rho_i^2(r) = -\rho_{00} a_{0i} \sinh \frac{R_{0i}}{a_{0i}} \frac{d}{dR_{0i}} \frac{\rho_i(r)}{\sinh \frac{R_{0i}}{a_{0i}}}, \quad (13)$$

we get

$$I_{11} = -4\pi \rho_{00} a_{01} \sinh \frac{R_{01}}{a_{01}} \frac{d}{dR_{01}} \frac{1}{\sinh \frac{R_{01}}{a_{01}}} \int_0^\infty \rho_1(p) \rho_2(p) j_0(pR) p^2 dp, \quad (14a)$$

$$I_{12} = -(4\pi)^2 \xi_2 \rho_{00} a_{01} R_{02} \beta_2 \sinh \frac{R_{01}}{a_{01}} Y_{20}(\Omega_2)$$

$$\begin{aligned}
& \times \frac{d}{dR_{01}} \frac{1}{\sinh \frac{R_{01}}{a_{01}}} \int_0^\infty dp p^2 j_2(pR) \rho_1(p) \int_0^\infty dr r^2 j_2(pr) \frac{d\hat{\rho}_2(r)}{dR_{02}} \\
& = -(4\pi)^2 \xi_2 \rho_{00}^2 a_{01} R_{02} \beta_2 \sinh \frac{R_{01}}{a_{01}} Y_{20}(\Omega_2) \frac{d}{dR_{01}} \frac{1}{\sinh \frac{R_{01}}{a_{01}}} \int_0^\infty dp p j_2(pR) \rho_1(p) \\
& \times \left[\frac{3}{\rho_{00} p^2} G_{12} - \frac{\pi b_{02}}{\sinh(\pi b_{02} p)} (p \pi b_{02} \cos(pR_{02}) \coth(\pi b_{02} p) + p R_{02} \sin(pR_{02}) + 2 \cos(pR_{02})) \right], \tag{14b}
\end{aligned}$$

$$\begin{aligned}
I_{13} & = (4\pi)^2 \xi_1' \beta_1 R_{01} Y_{20}(\Omega_1) \int_0^\infty dp p^2 j_2(pR) \rho_2(p) \int_0^\infty dr r^2 j_2(pr) \frac{d\hat{\rho}_1^2(r)}{dR_{01}} \\
& = (4\pi)^2 \xi_1' \beta_1 R_{01} b_{01}' Y_{20}(\Omega_1) \\
& \times \frac{d}{dR_{01}} \int_0^\infty dp p j_2(pR) \rho_2(p) \left[\frac{3}{b_{01}' p^2} G_{13} - \frac{\pi b_{01}'}{\sinh(\pi b_{01}' p)} \left\{ - \left(\pi b_{01}' \coth(\pi b_{01}' p) + \frac{3}{p} \right) \right. \right. \\
& \left. \left. \times \left(p \cos(pR_{01}) - \frac{\sin(pR_{01})}{b_{01}'} \coth \frac{R_{01}}{b_{01}'} \right) + \cos(pR_{01}) \left(1 - \frac{R_{01}}{b_{01}'} \coth \frac{R_{01}}{b_{01}'} \right) - p R_{01} \sin(pR_{01}) \right] \right], \tag{14c}
\end{aligned}$$

where

$$\rho_i(p) = \frac{\sqrt{2\pi} a_{0i} R_{0i} \rho_{00}}{p \sinh(\pi a_{0i} p)} \left(\frac{\pi a_{0i}}{R_{0i}} \sin(pR_{0i}) \coth(\pi a_{0i} p) - \cos(pR_{0i}) \right)$$

is the Fourier transformation of (7). The results of calculations of G_{12} and G_{13} are given in Appendix. The assumption of small overlap of the interacting nuclei leads to the simplified calculations of integrals:

$$I_{14} \simeq \frac{R_{02}^2}{2} \xi_2 \beta_2^2 Y_{20}^2(\alpha_2) \frac{d^2}{dR_{02}^2} \tilde{I}_{11}^{(2)}, \tag{14d}$$

$$I_{15} \simeq R_{01} R_{02} \xi_1' \xi_2 \beta_1 \beta_2 Y_{20}(\alpha_1) Y_{20}(\alpha_2) \frac{d^2}{dR_{01} dR_{02}} \tilde{I}_{11}, \tag{14e}$$

$$I_{16} \simeq \frac{R_{01}^2}{2} \xi_1' \beta_1^2 Y_{20}^2(\alpha_1) \frac{d^2}{dR_{01}^2} \tilde{I}_{11}^{(1)}, \tag{14f}$$

$$I_{17} \simeq \frac{R_{01} R_{02}^2}{2} \xi_1' \xi_2 \beta_1 \beta_2^2 Y_{20}(\alpha_1) Y_{20}^2(\alpha_2) \frac{d^3}{dR_{01} dR_{02}^2} \tilde{I}_{11}, \tag{14g}$$

$$I_{18} \simeq \frac{R_{01}^2 R_{02}}{2} \xi_1' \xi_2 \beta_1^2 \beta_2 Y_{20}^2(\alpha_1) Y_{20}(\alpha_2) \frac{d^3}{dR_{01}^2 dR_{02}} \tilde{I}_{11}, \tag{14i}$$

$$I_{19} \simeq \frac{R_{01}^2 R_{02}^2}{2} \xi_1' \xi_2 \beta_1^2 \beta_2^2 Y_{20}^2(\alpha_1) Y_{20}^2(\alpha_2) \frac{d^4}{dR_{01}^2 dR_{02}^2} \tilde{I}_{11}. \tag{14j}$$

The main approximation in (14d–14j) is the replacement of spherical functions in the integrands by their values at $\theta_i' = \alpha_i$. The expression for \tilde{I}_{11} coincides with the one

for I_{11} where ρ_1^2 and ρ_2 are replaced by $\tilde{\rho}_1^2$ and $\tilde{\rho}_2$, respectively. In contrast to I_{11} , $\tilde{I}_{11}^{(1)}$ contains $\tilde{\rho}_1^2$ instead of ρ_1^2 and $\tilde{I}_{11}^{(2)}$ contains $\tilde{\rho}_2$ instead of ρ_2 . Therefore, the calculations of \tilde{I}_{11} , $\tilde{I}_{11}^{(1)}$ and $\tilde{I}_{11}^{(2)}$ are similar to the calculation of I_{11} .

To obtain I_{11} , we should calculate the simple integral. If a_{01}/a_{02} is not representable as the ratio of two integers, then calculating the residues at poles we get for $R > R_{01} + R_{02}$:

$$\begin{aligned}
I_{11} = & -8\pi\rho_{00}^3 \frac{a_{01}^2 a_{02}}{R} \sinh \frac{R_{01}}{a_{01}} \frac{d}{dR_{01}} \frac{1}{\sinh \frac{R_{01}}{a_{01}}} \\
& \times \left[\frac{1}{a_{02}} \sum_{n=1}^{\infty} \frac{(-1)^n}{n} e^{-\frac{nR}{a_{01}}} \sinh \frac{R_{01}n}{a_{01}} \left\{ \left(R_{02}^2 T_1^{(1)} + \left(\frac{a_{01}}{n} + R \right) T_1^{(2)} + 2T_1^{(3)} \right) \sinh \frac{R_{02}n}{a_{01}} \right. \right. \\
& \left. \left. - R_{02} \left(\left(R + \frac{a_{01}}{n} \right) T_1^{(1)} + 2T_1^{(2)} \right) \cosh \frac{R_{02}n}{a_{01}} \right\} + 1 \longleftrightarrow 2 \right]. \quad (15)
\end{aligned}$$

At $R < R_{01} + R_{02}$ we obtain

$$\begin{aligned}
I_{11} = & 2\pi\rho_{00}^3 \frac{a_{01}^2 a_{02}}{R} \sinh \frac{R_{01}}{a_{01}} \frac{d}{dR_{01}} \frac{1}{\sinh \frac{R_{01}}{a_{01}}} \left[\frac{1}{a_{02}} \sum_{n=1}^{\infty} \frac{(-1)^n}{n} \right. \\
& \times \left\{ e^{-\frac{n(R_{01}+R_{02}-R)}{a_{01}}} \left[R_{02} \left(-R + \frac{a_{01}}{n} + R_{02} \right) T_1^{(1)} + \left(-R + \frac{a_{01}}{n} + 2R_{02} \right) T_1^{(2)} + 2T_1^{(3)} \right] \right. \\
& + e^{-\frac{n(R+R_{01}-R_{02})}{a_{01}}} \left[R_{02} \left(-R - \frac{a_{01}}{n} + R_{02} \right) T_1^{(1)} + \left(R + \frac{a_{01}}{n} - 2R_{02} \right) T_1^{(2)} + 2T_1^{(3)} \right] \\
& \left. + e^{-\frac{n(R-R_{01}+R_{02})}{a_{01}}} \left[R_{02} \left(R + \frac{a_{01}}{n} + R_{02} \right) T_1^{(1)} + \left(R + \frac{a_{01}}{n} + 2R_{02} \right) T_1^{(2)} + 2T_1^{(3)} \right] \right\} \\
& \left. + 1 \longleftrightarrow 2 - T^{(0)} \right] \quad (16)
\end{aligned}$$

Here the following notations are used:

$$\begin{aligned}
T^{(0)} = & \frac{1}{6a_{01}a_{02}} \left[2R \left((R_{01} + R_{02})^3 - 3(R_{01} + R_{02})R_{01}R_{02} + a_{01}^2 R_{01} + a_{02}^2 R_{02} \right) \right. \\
& - \frac{7}{20}\pi^4 (a_{01}^4 + a_{02}^4) + \frac{1}{6}\pi^4 a_{01}^2 a_{02}^2 + \pi^2 (R_{01}^2 - R_{02}^2) (a_{02}^2 - a_{01}^2) \\
& - \frac{1}{2}\pi^2 (a_{01}^2 + a_{02}^2) \left(R^2 + 2R_{01}R_{02} + (R_{01} - R_{02})^2 \right) \\
& - 3R_{01}R_{02} \left(R^2 + (R_{01} - R_{02})^2 \right) - \left(3R^2 + (R_{01} - R_{02})^2 \right) (R_{01} - R_{02})^2 \\
& \left. + \frac{1}{8} \left((R + R_{01} - R_{02})^4 + (R - R_{01} + R_{02})^4 \right) \right] \quad (17)
\end{aligned}$$

and

$$T_i^{(1)} = \frac{\pi a_{0j}}{\sin(\pi n a_{0j}/a_{0i})},$$

$$\begin{aligned}
T_i^{(2)} &= \frac{\pi^2 a_{0j}^2}{\sin^2(\pi n a_{0j}/a_{0i})} \cos(\pi n a_{0j}/a_{0i}), \\
T_i^{(3)} &= \frac{\pi^3 a_{0j}^3}{2} \frac{1 + \cos^2(\pi n a_{0j}/a_{0i})}{\sin^3(\pi n a_{0j}/a_{0i})},
\end{aligned} \tag{18}$$

where $i, j = 1, 2$ and $i \neq j$. The sums in (15) and (16) converge quickly except for the immediate neighbourhood of $R = R_{01} + R_{02}$. In this case the numerical integration in (14a) is needed.

At $a_{01} = a_{02} = a$ the expression (15) transforms into

$$\begin{aligned}
I_{11} &= -\frac{4\pi}{3} \rho_{00}^3 \frac{a^2}{R} \sinh \frac{R_{01}}{a} \frac{d}{dR_{01}} \frac{1}{\sinh \frac{R_{01}}{a}} \sum_{n=1}^{\infty} \frac{1}{n} e^{-\frac{nR}{a}} \\
&\times \left\{ \left[R^3 + \frac{3a}{n} \left(R^2 + \frac{2Ra}{n} + \frac{2a^2}{n^2} \right) - 3a^2 \left(R + \frac{a}{n} \right) \left(\frac{2\pi^2}{3} + \frac{R_{01}^2 + R_{02}^2}{a^2} \right) \right] \right. \\
&\times \sinh \frac{nR_{01}}{a} \sinh \frac{nR_{02}}{a} + 2R_{01}(\pi^2 a^2 + R_{01}^2) \cosh \frac{nR_{01}}{a} \sinh \frac{nR_{02}}{a} \\
&\left. + 2R_{02}(\pi^2 a^2 + R_{02}^2) \sinh \frac{nR_{01}}{a} \cosh \frac{nR_{02}}{a} \right\}, \tag{19}
\end{aligned}$$

and (16) transforms into

$$\begin{aligned}
I_{11} &= \frac{\pi}{3} \rho_{00}^3 \frac{a^2}{R} \sinh \frac{R_{01}}{a} \frac{d}{dR_{01}} \frac{1}{\sinh \frac{R_{01}}{a}} \left[\sum_{n=1}^{\infty} \frac{1}{n} \left\{ e^{-\frac{n(R_{01}+R_{02}-R)}{a}} D(-R, R_{01}, R_{02}) \right. \right. \\
&\left. \left. + e^{-\frac{n(R+R_{01}-R_{02})}{a}} D(R, R_{01}, -R_{02}) + e^{-\frac{n(R-R_{01}+R_{02})}{a}} D(R, -R_{01}, R_{02}) \right\} - T^{(0)} \right], \tag{20}
\end{aligned}$$

where

$$\begin{aligned}
D(R, R_{01}, R_{02}) &= R^3 - (R_{01} + R_{02})^2 (3R + 2(R_{01} + R_{02})) \\
&+ \frac{3a}{n} \left(R^2 - (R_{01} + R_{02})^2 + \frac{2aR}{n} + \frac{2a^2}{n^2} \right) \\
&+ 6 \left(R + R_{01} + R_{02} + \frac{a}{n} \right) \left(R_{01} R_{02} - \frac{\pi^2 a^2}{3} \right).
\end{aligned}$$

The sums in (15) and (19) coincide with the corresponding sums in [14] if $\sinh(R_{0i}n/a_{0i})$ is replaced by $0.5 \exp(R_{0i}n/a_{0i})$. In (16) and (20) the terms, which are proportional to $\exp(-n(R + R_{01} + R_{02})/a_{0i})$, were neglected.

The integrals in (14b) and (14c) can be calculated in the same manner as in (14a). By using the expressions (14d–14j) the contribution of terms I_{1k} ($k = 4, \dots, 9$) to I_1 can be obtained. The integral

$$I_2 = \int \rho_1(\mathbf{r}) \rho_2^2(\mathbf{r} - \mathbf{R}) d\mathbf{r} \tag{21}$$

in (5) results from (12) by replacing index 1 by 2 and vice versa. The calculation of the integral

$$I_3 = \int \rho_1(\mathbf{r})\rho_2(\mathbf{r} - \mathbf{R})d\mathbf{r} \quad (22)$$

reduces to the calculation of integrals which differ from (12) by the replacement of ρ_1^2 , $\tilde{\rho}_1^2$ and ξ_1' by ρ_1 , $\tilde{\rho}_1$ and ξ_1 , respectively. Thus, the presented expressions allow us to calculate $U_N(R)$ if the nucleon density is chosen in the form (6) or (7).

2.2 INTERACTION OF LIGHT AND HEAVY NUCLEI AND TWO LIGHT NUCLEI

As it was noted before, for light nuclei the nucleon density is taken in the form (8). In the further consideration of asymmetric DNS we shall suppose that a light nucleus has a spherical shape ($\beta_1 = 0$). Therefore, to obtain $U_N(R)$, the integrals I_{11} , I_{12} and I_{14} should be calculated.

At $\beta_2 = 0$ we get

$$\begin{aligned} U_N(R) = & 2C_0A_1 \left(\frac{\gamma^2}{\pi}\right)^{1/2} e^{-\gamma^2R^2} \frac{1}{R} \int_0^\infty e^{-\gamma^2r^2} \frac{\rho_2(r)}{\rho_{00}} \\ & \times \left[(F_{in} - F_{ex}) \left(\rho_2(r) \sinh(2\gamma^2Rr) + \frac{A_1}{4} \left(\frac{\gamma^2}{\pi}\right)^{3/2} e^{-\gamma^2(r^2+R^2)} \sinh(4\gamma^2Rr) \right) \right. \\ & \left. + \rho_{00}F_{ex} \sinh(2\gamma^2Rr) \right] r dr. \quad (23) \end{aligned}$$

For $\beta_2 \neq 0$ the integral I_{11} is calculated as in (23). The integrals in (12) can be reduced to the first order integrals

$$I_{12} = 4\pi A_1 \xi_2 \beta_2 R_{02} \left(\frac{\gamma^2}{\pi}\right)^3 Y_{20}(\Omega_2) \int_0^\infty e^{-2\gamma^2(r^2+R^2)} \sqrt{\frac{\pi}{8\gamma^2rR}} I_{5/2}(4\gamma^2rR) \frac{d\tilde{\rho}_2}{dR_{02}} r^2 dr, \quad (24)$$

$$\begin{aligned} I_{14} = & 5A_1 \frac{R_{02}}{2} \xi_2 \beta_2^2 \left(\frac{\gamma^2}{\pi}\right)^3 \sum_{L=0,2,4} \sqrt{\frac{4\pi}{2L+1}} (C_{2020}^{L0})^2 Y_{20}(\Omega_2) \\ & \times \int_0^\infty e^{-2\gamma^2(r^2+R^2)} \sqrt{\frac{\pi}{8\gamma^2rR}} I_{L+1/2}(4\gamma^2rR) \frac{d^2\tilde{\rho}_2}{dR_{02}^2} r^2 dr. \quad (25) \end{aligned}$$

Here $I_{L+1/2}(z)$ is the modified Bessel function, C_{2020}^{L0} is the Clebsh-Gordan coefficient. By evident replacements in (24) and (25) the expressions for I_{22} , I_{24} , I_{32} and I_{34} can be easily obtained.

Interaction of two light nuclei is described by the simple analytical expression for I_1

$$I_1 = \pi A_1^2 A_2 \left(\frac{\gamma_1^2}{\pi} \right)^3 \left(\frac{\gamma_2^2}{\pi} \right)^{3/2} \frac{\sqrt{\pi}}{(2\gamma_1^2 + \gamma_2^2)^{3/2}} \exp \left(-\frac{2\gamma_1^2 \gamma_2^2}{2\gamma_1^2 + \gamma_2^2} R^2 \right). \quad (26)$$

Similar expressions are obtained for I_2 and I_3 . Note that the results of this subsection are useful when instead of (8) we take the dependence

$$\begin{aligned} \rho_1(r) &= \frac{A_1}{4} \left(\frac{\gamma_1^2}{\pi} \right)^{3/2} (1 + 2\gamma_1^2 r^2) \exp(-\gamma_1^2 r^2) \\ &= \frac{A_1}{4} \left(\frac{\gamma_1^2}{\pi} \right)^{3/2} \left(1 - 2\gamma_1^2 \frac{d}{d(\gamma_1^2)} \right) \exp(-\gamma_1^2 r^2) \end{aligned}$$

suggested for ^{16}O [11].

2.3 COULOMB AND CENTRIFUGAL POTENTIALS

The Coulomb potential for two deformed nuclei

$$U_{\text{coul}}(R) = e^2 Z_1 Z_2 \int \frac{\rho_1^{\tilde{z}}(\mathbf{r}_1) \rho_2^{\tilde{z}}(\mathbf{r}_2)}{|\mathbf{r}_1 - \mathbf{r}_2|} d\mathbf{r}_1 d\mathbf{r}_2 = \frac{2e^2 Z_1 Z_2}{(2\pi)^2} \int e^{i\mathbf{p}\mathbf{R}} \frac{1}{p^2} \rho_1^{\tilde{z}}(\mathbf{p}) \rho_2^{\tilde{z}}(-\mathbf{p}) d\mathbf{p}. \quad (27)$$

can be calculated analytically by neglecting the diffuseness of the charge distributions $\rho_1^{\tilde{z}}$ and $\rho_2^{\tilde{z}}$. In this case the Fourier transforms $\rho_i^{\tilde{z}}(\mathbf{p})$ have a simple form. For $R > R_{01} + R_{02}$ the same expression can be obtained as in [15]. Since the expression for $U_{\text{coul}}(R)$ is cumbersome for $R < R_{01} + R_{02}$, we do not write it here. Note also the possibility to take into account only terms of the first order in β_i in the expansion of $\rho_i^{\tilde{z}}$ [16].

If the sticking condition is valid, the DNS rotational energy can be written as

$$U_{\text{rot}}(R) = \frac{\hbar^2 J(J+1)}{2(j_1 + j_2 + \mu R^2)}, \quad (28)$$

where J is the total angular momentum of the system, j_i are the moments of inertia of each nucleus. The values of j_i are known for axial and quadrupole deformed nuclei considered in this paper.

3. Relationship of double folding potential with proximity potential

Using (13) we can approximately rewrite (5) for the spherical nuclei as

$$U_N(R) \approx C_0 \left\{ (F_{\text{in}} - F_{\text{ex}}) \left(2 - a_{01} \frac{\partial}{\partial R_{01}} - a_{02} \frac{\partial}{\partial R_{01}} \right) + F_{\text{ex}} \right\} \int \rho_1(r) \rho_2(r - \mathbf{R}) dr. \quad (29)$$

Let us consider the case $a_{01} = a_{02} = a$. Then, from (19) and (29), for $R > R_{01} + R_{02}$ we get the approximate expression:

$$\begin{aligned}
U_N(R) \approx & 2\pi\rho_{00}^2 C_0 a^2 \frac{R_{01} R_{02}}{R} \left\{ \sum_{n=1}^{\infty} e^{-n\delta} \left[\frac{2F_{in} - F_{ex}}{n^2} (1 + n\delta) - 2(F_{in} - F_{ex})\delta \right] \right. \\
& + \frac{R_0^2}{2R_{01} R_{02} R_0} a \sum_{n=1}^{\infty} e^{-n\delta} \left[\frac{2F_{in} - F_{ex}}{n^3} (2 + 2n\delta + n^2\delta^2) \right. \\
& \left. \left. - \frac{2(F_{in} - F_{ex})}{n^2} (1 + n\delta + n^2\delta^2) \right] \right. \\
& + \frac{R_0^2}{6R_{01} R_{02}} \left(\frac{a}{R_0} \right)^2 \sum_{n=1}^{\infty} e^{-n\delta} \left[\frac{2F_{in} - F_{ex}}{n^4} \right. \\
& \times (6 + 6n\delta + 3n^2\delta^2 + n^3\delta^3 - 2\pi^2 n^3\delta - 2\pi^2 n^2) \\
& \left. \left. - \frac{2(F_{in} - F_{ex})}{n^3} (6 + 6n\delta + 3n^2\delta^2 + n^3\delta^3 - 2\pi^2 n^3\delta) \right] \right\}. \quad (30)
\end{aligned}$$

In (30) the terms of order $\exp(-nR_{0i}/a)$ have been neglected, $\delta = (R - R_{01} - R_{02})/a$ and $R_0 = R_{01} + R_{02}$. Let us denote the expression in braces by

$$\Phi(\delta) = \Phi_0(\delta) + \frac{R_0^2}{2R_{01} R_{02} R_0} a \Phi_1(\delta) + \frac{R_0^2}{6R_{01} R_{02}} \left(\frac{a}{R_0} \right)^2 \Phi_2(\delta), \quad (31)$$

where Φ_0 , Φ_1 and Φ_2 are the first, second and third sums in (30), respectively. At $F_{in} = F_{ex} = 1$ these sums coincide with the corresponding sums obtained in [17] where the single folding potential has been calculated. The functions Φ_0 , Φ_1 and Φ_2 are the same for any pair of interacting nuclei if we suppose $F_{in,ex} = f_{in,ex}$. For example, in [17] the following expression for the universal function Φ_0

$$\Phi_0(\delta) = \sum_{n=1}^{\infty} e^{-n\delta} \frac{1 + n\delta}{n^2},$$

has been obtained which differs from our result by the factor after the exponential.

Thus, the double folding potential can be expressed in the form of the proximity potential but with another universal function. The sign in (30) depends on the sign of $\Phi(\delta)$. In Fig.2 the function $\Phi_0(\delta)$ is compared with the universal function of the proximity potential [4]. For $\delta < \delta_{min} = 0.15$ the function $\Phi_0(\delta)$ increases with decreasing δ . This leads to formation of the repulsive core in $U_N(R)$. By using (20) and (29) the universal functions can be obtained for $\delta < 0$. Their expressions are cumbersome and are not given here. The function $\Phi_0(\delta)$ is an approximately linear function of δ at large negative δ . The universal function of the proximity potential has the same kind of behavior. The comparison of the universal functions of the double folding and

proximity potentials (Fig.2) demonstrates a smaller depth of the first. However, the difference of these potentials is not essential when $R > R_b$.

The case of small deformations of nuclei makes it necessary to change geometrical factors in (30) by using the following substitution

$$R_{0i} \rightarrow R_{0i}(1 + \beta_i Y_{20}(\alpha_i)).$$

It is assumed that the universal functions depend on the minimum distance δ between the surfaces of nuclei [18].

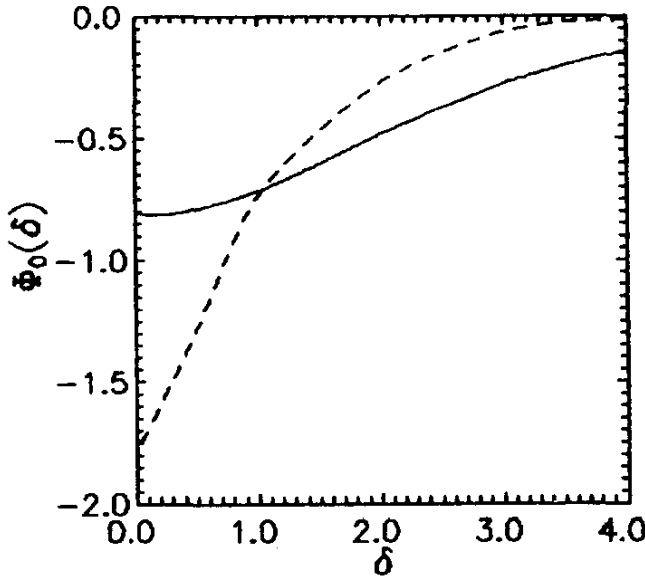


Fig.2. Universal functions $\Phi_0(\delta)$ for proximity potential (dashed line) and double folding potential proposed by us (solid line)

4. Results of calculations

By using the expressions obtained above the nucleus-nucleus potentials for the entrance channels of few reactions have been calculated (Fig.3). A spherical nuclear shape has been assumed in these calculations. The set of parameters $C_0 = 300 \text{ MeV fm}^3$, $f_{in} = 0.09$, $f_{ex} = -2.59$, $f'_{in} = 0.42$ and $f'_{ex} = 0.54$ has been used [8]. A good description of the position (R_b) and height (E_b) of the entrance potential barrier [19,20] can be obtained by a small variation of the parameters $r_0 = (1.10 \div 1.15) \text{ fm}$ and $a_0 = (0.50 \div 0.55) \text{ fm}$ in (6). The dependences $U(R)$ on R for few reactions are presented in Fig.3 at different values of J . In the case of massive systems the potential pocket in $U(R)$ either has a small depth or is absent because of the strong Coulomb repulsion. However, due to the nucleon exchange between the interacting nuclei the potential pocket becomes deeper [21]. Therefore, to evaluate the stability of the massive DNS, this effect should be taken into account.

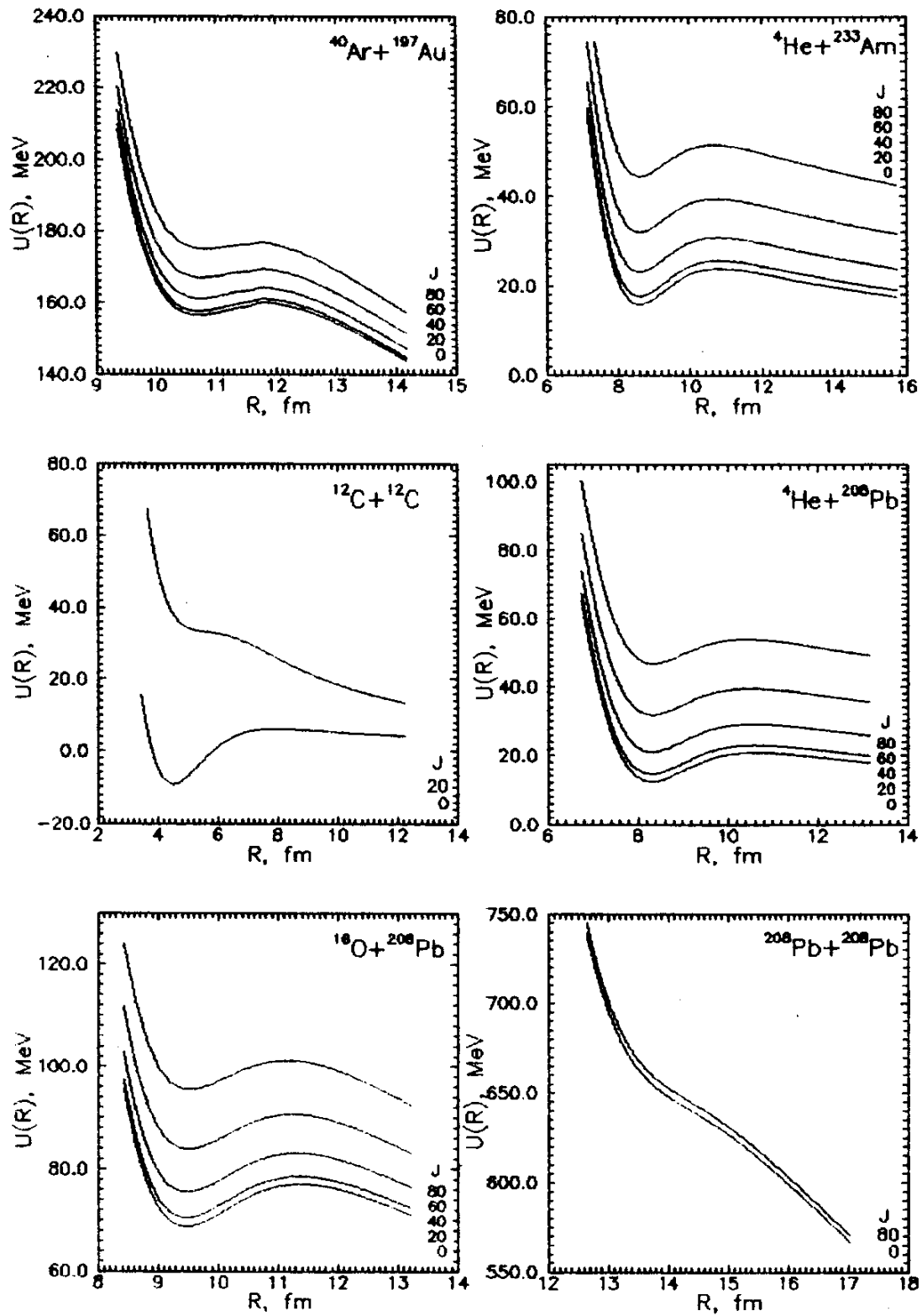


Fig.3. Dependence of nucleus-nucleus potentials on R and J for various combinations of nuclei

To calculate the interaction both between the light and heavy nuclei and between the two light nuclei, the formulae of subsection 2.2 have been used. We have chosen $\gamma = 0.671 \text{ fm}^{-1}$ for the α -particle. It corresponds to the minimization of the total α -particle energy in the density functional [12]. The values of γ for other light nuclei have been obtained by fitting empirical values of E_b and R_b [19,20]. One should note the strong dependence of the potential pocket depth on γ .

The comparison of $U(R)$ for the systems $^{40}\text{Ar}+^{197}\text{Au}$ and $^4\text{He}+^{233}\text{Am}$ (Fig.3) shows the increase in the potential pocket depth with increasing asymmetry of the DNS. The same behavior is observed for other forms of the potentials.

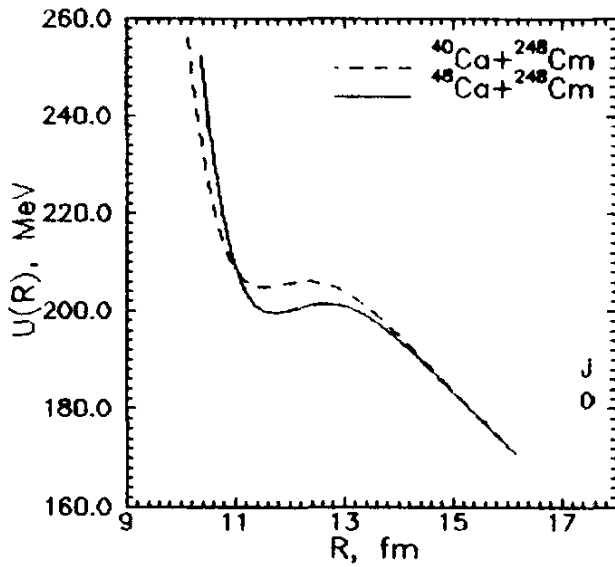


Fig.4. Dependence of nucleus-nucleus potentials on R for the reactions $^{40}\text{Ca}+^{248}\text{Cm}$ and $^{48}\text{Ca}+^{248}\text{Cm}$ at $J = 0$

To demonstrate the influence of neutron excess on the potential $U(R)$, the calculations for the reactions $^{40}\text{Ca}+^{248}\text{Cm}$ and $^{48}\text{Ca}+^{248}\text{Cm}$ have been done (Fig.4). It is seen that the value of E_b is smaller for the reaction with ^{48}Ca . The entrance potential barrier can decrease with increasing neutron excess in the colliding nuclei due to the soft dipole mode [22,23]. This mode corresponds to a dipole oscillation of the excess neutrons with respect to the nucleus core. The excitation energy of the soft mode can be estimated in the following way [23]

$$\hbar\omega_{pr} \sim \left[\frac{Z(N - N_c)}{N(Z + N_c)} \right]^{1/2} 80/A^{1/3} \text{ MeV.}$$

where N_c is the neutron number of the core. Knowing $\hbar\omega_{pr}$, it is possible to estimate the expectation value of the square of the neutron excess displacement with respect to the core $\bar{\Delta}^2$. Assuming that the total nucleon density is constant, one can obtain the value of the change V_c of the entrance barrier due to the soft dipole mode. For the reaction $^{54}\text{Ca}+^{144}\text{Sm}$ we have obtained $\sqrt{\bar{\Delta}^2} \approx 0.46 \text{ fm}$ and $V_c = 4.8 \text{ MeV}$. In our

calculation the unchangeable $U_N(R)$ has been used. From the above arguments the great enhancement of sub-barrier fusion is expected at this value of V_c .

It is known that the exit potential barrier differs from the entrance one [24,25] due to the change of deformation of the nuclei during their interaction. The calculated $U(R)$ for the system ${}^4\text{He}+{}^{233}\text{Am}$ is presented in Fig.5. Due to the deformation of a heavy nucleus ($\beta = 0.45$) the decrease of E_b is about 15% at $\Omega_1 = \Omega_2 = 0$. The same decrease of the emission barrier of the α -particle in the reaction ${}^{40}\text{Ar}+{}^{197}\text{Au}$ is observed [24,25] in comparison with the fusion barrier of nuclei ${}^4\text{He}$ and ${}^{233}\text{Am}$. It should be noted that the influence of deformation on the potential form is small. The width and depth of the potential pocket are not changed essentially.

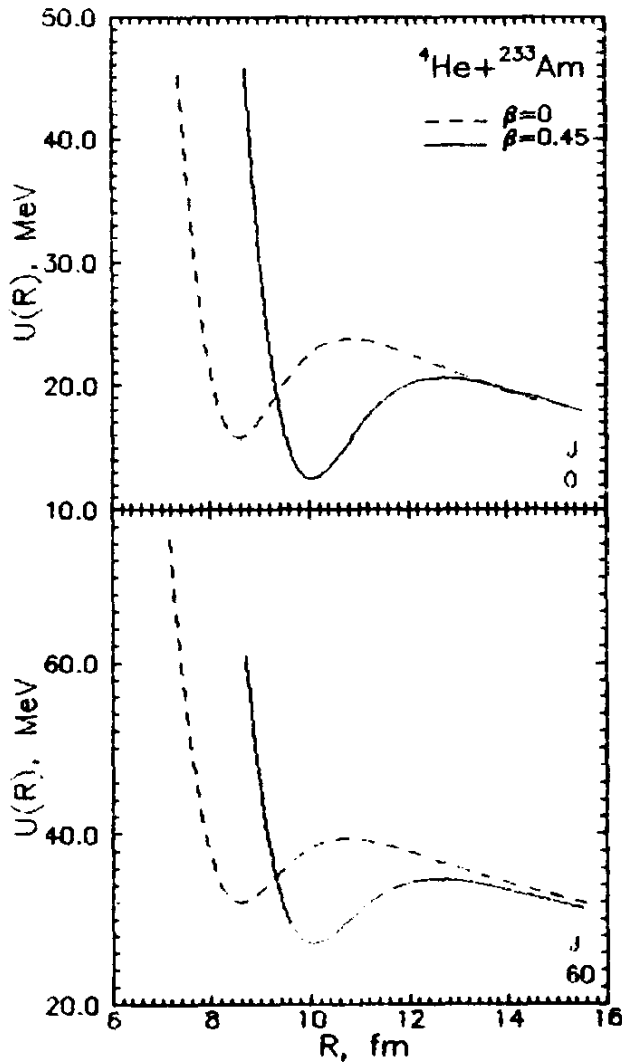


Fig.5. Dependence of nucleus-nucleus potential on R for the system ${}^4\text{He}+{}^{233}\text{Am}$ at $J = 0$ and $J = 60$. Calculated results for spherical and deformed heavy nucleus are presented by dashed and solid lines, respectively

The dependence of $U(R)$ on various orientations of nuclei is presented in Fig.6 for the system ${}^{238}\text{U}+{}^{238}\text{U}$, $\beta_1 = \beta_2 = 0.26$. As one can see, for the touching nuclei the nose to nose configuration is energy preferable.

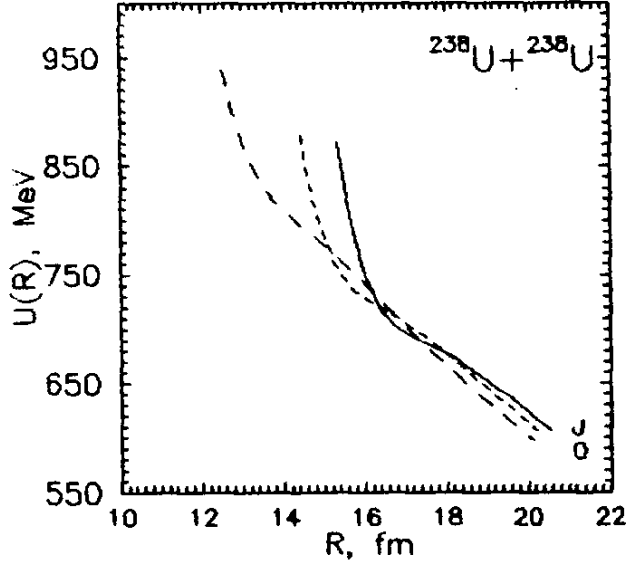


Fig.6. Dependence of nucleus-nucleus potential on R and orientations of nuclei for the system $^{238}\text{U}+^{238}\text{U}$, $\beta_1 = \beta_2 = 0.26$, at $J = 0$. Calculated results for $\Omega_1 = 0$ and $\Omega_2 = \pi$, $\Omega_1 = \pi/4$ and $\Omega_2 = 3\pi/4$, $\Omega_1 = \pi/2$ and $\Omega_2 = \pi/2$ are presented by solid line, short dashed line and long dashed line, respectively

The dependences of the DNS potential energy

$$V(R, Z, J) = U(R, Z, J) + B_1 + B_2 - (B_{12} + E_{rot}(J)) \quad (32)$$

on the charge of one nucleus and J are presented in Fig.7 for the systems $^{58}\text{Ni}+^{58}\text{Ni} \rightarrow ^{116}\text{Ba}$ and $^{76}\text{As}+^{76}\text{As} \rightarrow ^{152}\text{Dy}$. The value of R for each Z corresponds to the position of the potential pocket minimum. The mass numbers of nuclei have been chosen by minimization of (32). For convenience, we have normalized (32) to the energy of a rotating compound nucleus ($B_{12} + E_{rot}(J)$). The binding energies B_1 , B_2 and B_{12} have been taken from [26,27].

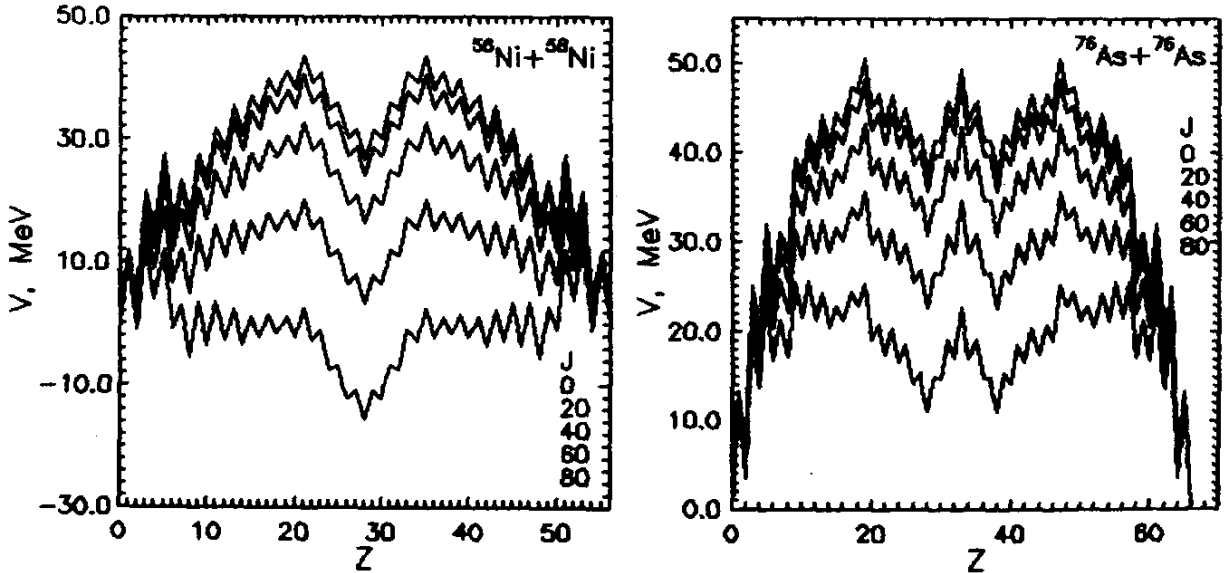


Fig.7. Dependence of the DNS potential energy on charge Z of one nucleus and J for the systems $^{58}\text{Ni}+^{58}\text{Ni}$ and $^{76}\text{As}+^{76}\text{As}$

At high values of J the energy of the symmetric configuration seems to be close to the energy of a compound nucleus. The semiaxes ratio of the equivalent ellipsoid is approximately equal to 2 : 1. This ratio characterizes the superdeformed states of the nuclei. Therefore, the relationship between the superdeformed nuclei and symmetrical DNS can be assumed. The symmetrical DNS transforms probably into a superdeformed mononucleus with increasing neck between the DNS nuclei.

If we consider neutron deficient nuclei far from stability which have relatively small binding energies, then some of their excited states can be imagined as formed by two strongly bound interacting fragments. Constituent fragments are strongly bound because, being lighter, they have such an N/Z -ratio that corresponds to large binding energies. Due to the balance in binding energies these cluster-type states can appear at relatively low excitation energies. The investigation of the relationship between the DNS configurations and exotic nuclear shapes is a separate interesting problem.

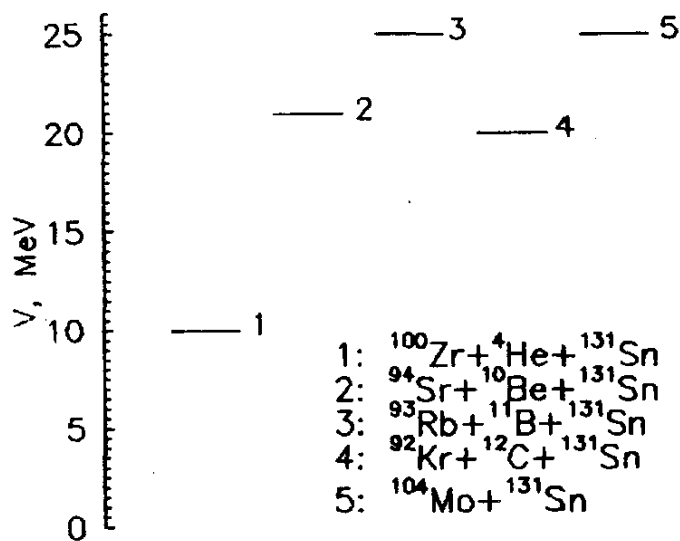


Fig.8. Potential energies of some trinuclear systems formed of the excited nucleus ^{235}U . Potential energy of the corresponding DNS is presented as well

The experimental observation of the emission of light nuclei from the contact region of two heavy nuclei [6] can be considered as an indication of the existence of trinuclear systems. For example, the ^{12}C emission from the neck can be interpreted as the decay of a trinuclear system. The potential energies of the trinuclear systems formed of the excited nucleus ^{235}U are presented in Fig.8. It is seen that the energies of some trinuclear systems are smaller than the energy of the corresponding DNS. Therefore, in the contact region of two massive nuclei the light nucleus formation is possible.

5. Summary

The analytical expressions have been obtained to calculate the nuclear part of the nucleus-nucleus potential in the double folding form. The relationship of this potential with proximity potential has been found. The influence of deformation and orientation of the nuclei on the interaction potential has been investigated. The decrease of the interaction barrier with increasing neutron excess in one nucleus has been demonstrated. Due to the balance in binding energies the excited states of some nuclei can be imagined as dinuclear or trinuclear systems. The proposed calculation method of the DNS potential energy can be used at any of its mass (charge) asymmetries.

Appendix

Upon calculating the residues at poles, the integrals

$$G_{12} = \int_0^{\infty} \frac{\sin(pr)}{r} \frac{d\tilde{\rho}_2(r)}{dR_{02}} dr,$$

$$G_{13} = \int_0^{\infty} \frac{\sin(pr)}{r} \frac{dr}{(1 + \exp((r - R_{01})/b'_{01}))^2}$$

can be represented by the following sums:

$$G_{12} = \pi \rho_{00} \left\{ \frac{\exp(-R_{02}/b_{02})}{b_{02}(1 + \exp(-R_{02}/b_{02}))^2} - 2b_{02} \sum_{n=0}^{\infty} \frac{\exp(-\pi p b_{02}(2n+1))}{R_{02}^2 + (\pi b_{02})^2(2n+1)^2} \right. \\ \times \left[-\frac{2R_{02}}{R_{02}^2 + (\pi b_{02})^2(2n+1)^2} (R_{02} \cos(pR_{02}) + \pi b_{02}(2n+1) \sin(pR_{02})) \right. \\ \left. \left. + (\pi b_{02} p(2n+1) + 1) \cos(pR_{02}) - pR_{02} \sin(pR_{02}) \right] \right\},$$

$$G_{13} = \pi \left\{ \frac{1}{(1 + \exp(-R_{01}/b'_{01}))^2} - \frac{1}{2} \operatorname{sgn}(p) + 2b'_{01} \sum_{n=0}^{\infty} \frac{\exp(-\pi p b'_{01}(2n+1))}{R_{01}^2 + (\pi b'_{01})^2(2n+1)^2} \right. \\ \times \left[\left(-\frac{b'_{01} R_{01}^2}{R_{01}^2 + (\pi b'_{01})^2(2n+1)^2} - R_{01} + b'_{01}{}^2 \pi p(2n+1) + \frac{b'_{01}{}^3 \pi^2 p(2n+1)^2}{R_{01}^2 + (\pi b'_{01})^2(2n+1)^2} \right) \right. \\ \left. \times \cos(pR_{01}) - \left(b'_{01} p R_{01} + \frac{2b'_{01}{}^2 \pi R_{01}(2n+1)}{R_{01}^2 + (\pi b'_{01})^2(2n+1)^2} + b'_{01} \pi(2n+1) \right) \sin(pR_{01}) \right] \right\}.$$

References

- 1) Volkov V.V.// Nuclear reactions of deep inelastic transfers. Moscow.: Energoizdat, 1982.
- 2) Bragin V.N., Zhukov M.V.// Particles & Nuclei. 1984. V. 15, P. 725.

- 3) Ngo Ch.// *Progr. Part. and Nucl. Phys.* 1986. V. 16. P. 139.
- 4) Blocki J. et al.// *Ann. Phys. (N.Y.)*, 1977. V. 105. P. 427.
- 5) Kadmsky S.G. et al.// *Sov. J. Nucl. Phys.* 1990. V. 51. P. 50.
- 6) Fields D.E. et al.// *Phys. Rev. Lett.* 1992. V. 69. P. 3713.
- 7) Antonenko N.V., Jolos R.V.// *Z. Phys.* 1991. V. A339. P. 453.
- 8) Migdal A.B.// *Theory of finite Fermi systems and applications to atomic nuclei.* Moscow: Nauka, 1988.
- 9) Beiner M. et al.// *Nucl. Phys.* 1975. V. A238. P. 29.
- 10) Volkov V.V.// *Proc. 6th Int. Conf. on Nuclear Reaction Mechanisms.* Italy, Varenna, 1991. P. 39.
- 11) Antonov A.N. et al.// *Nucleon momentum and density distributions in nuclei.* Oxford: Clarendon Press, 1988.
- 12) Manngard P. et al.// *Proc. 5th Int. Conf. on Nuclear Reaction Mechanisms.* Italy, Varenna, 1988. P. 385.
- 13) Satchler G.R., Love W.G.// *Phys. Rep.* 1979. V. 55. P. 183.
- 14) Goldfarb L.J.B.// *Nucl. Phys.* 1978. V. A301. P. 497.
- 15) Wong C.Y.// *Phys. Rev. Lett.* 1973. V. 31. P. 766.
- 16) Krappe H.J.// *Ann. Phys. (N.Y.)*, 1976. V. 99. P. 142.
- 17) Schechter H., Canto L.F.// *Nucl. Phys.* 1979. V. A314. P. 470.
- 18) Baltz A.J., Bayman B.F.// *Phys. Rev.* 1982. V. C26. P. 1969.
- 19) Birkelund J.R., Huizenga J.R.// *Phys. Rev.* 1978. V. C17. P. 126.
- 20) Vaz L.C. et al.// *Phys. Rep.* 1981. V. 69. P. 373.
- 21) Jolos R.V., Nasirov A.K.// *Sov. J. Nucl. Phys.* 1987. V. 45. P. 1298.
- 22) Dasso C.H., Donangelo R.// *Phys. Lett.* 1992. V. B276. P. 1.
- 23) Hussein M.S.// *Nucl. Phys.* 1991. V. A531. P. 192.

- 24) Alexander J.M. et al.// Z. Phys. 1982. V. A305. P. 313.
- 25) Vaz L.C. et al.// Z. Phys. 1983. V. A311. P. 89.
- 26) Wapstra A.M., Audi G.// Nucl. Phys. 1985. V. A432. P. 1.
- 27) Liran S., Zeldes N.// Atomic Data and Nucl.Data Tables. 1976. V. 17. P. 431.

This work was supported partly by the Russia Ministry of Education under Grant
2-61-13-28

**Received by Publishing Department
on November 10, 1993.**